PREDICTING PLASMA POLYMER DEPOSTION RATES FOR ACETALDEHYDE

Henry W. Oviatt, Ph.D.

Introduction

During my career I have worked on polymer surface modification and analysis within the field of biomaterials with the goal of improving biocompatibility. The general approach has been the surface modification of polymer surfaces of interest by radio frequency glow discharge surface functionalization, followed by derivatization of the surface with a biologically advantageous surface layer. Acetaldehyde in the past has been one of the plasma "monomers" of interest because it has a reactive functional aldehyde group that reacts readily with amines to form schiff bases, which can be subsequently reduced to a stable secondary or tertiary amine.[1,2] Aldehyde modified surfaces can then be functionalized with collagen or other amine containing molecules to create desirable cell adhesion properties, such as for synthetic corneal onlays used for refractive correction.[3]

Experimental

The configuration of the plasma reactor used has been previously described.[4,5] Briefly, experiments were performed using a capacitivly coupled radio frequency glow discharge (RFGD) apparatus.[5] The reactor consists of a cylindrical glass chamber (175 mm dia x 350 mm ht.) containing two vertical electrodes (90 x 18 mm separated by 16 mm). The lower electrode consists of a copper housing 10 cm diameter by 7.5 cm height for the quartz crystal microbalance (QCM), with the crystal of the balance set in the center of the lower electrode. The RFGD was powered by a commercial generator (ENI model HPG-2) operated at 200 kHz. The quartz crystal microbalance was a Maxtek Model TM-100 thickness monitor. Ancillary fittings, such as the pressure sensor (MKS Baratron), valves, and the pumping line, were standard items.

Samples were prepared by placing the substrate on the lower electrode, closing the system, and evacuating to the base pressure. The system was checked for leaks by monitoring the pressure rise with the isolated reaction chamber after the base pressure was reached and before the monomer flow was initiated. The monomer flow was

then adjusted using a stainless steel Nupro valve (Nupro SS-4BMG-VCR) to the desired pressure. In our reactor design the monomer vapor was introduced at the top of the reactor between the electrode rods and was exhausted out the bottom of the reactor chamber. When a stable monomer pressure was reached, hereafter referred to as the Equilibrium Monomer Pressure (EMP), the flow rate of the monomer was measured over a one minute period by isolating the reaction chamber from the vacuum source and monitoring the pressure rise with a Baratron pressure transducer in the absence of the vacuum pump and cold trap. Flow rates of gas at the base pressure were then converted to flow rates at STP using Equation 1[6],

$$F(STP) = V_{vac}\left(\frac{P_{vac}}{P_o}\right)\left(\frac{dP}{dt}\right)_{V,T} \qquad \text{(Equation 1)}$$

where F is the flow rate at STP (cm^3-torr-min^{-1}), V_{vac} is the volume of the reactor, P_{vac} is the EMP, P_o is atmospheric pressure, and $(dP/dt)_{VT}$ is the measured flow rate conducted at constant reactor volume and temperature. Plasma deposition rates in the form of QCM data were captured directly from the QCM signal generator through the use of Lab View™ software and an inhouse fabricated A/D interface system. Calibration of the QCM system was performed by correlating XPS analysis of plasma polymers on fluorinated ethylene-propylene (FEP) allowing the calculation of the thickness of deposited plasma polymers by the use of angle resolve spectra employing the F1s signal to determine the plasma polymer depth. Deposition parameters for the QCM were then used directly to measure the thickness of the plasma polymer on the QCM crystal.

Results

We were interested in understanding the variables in the plasma polymerization process and how they affect the resulting plasma polymers and deposition rates. To this end we incorporated a degree of automation in the lab scale reactor by incorporating a quartz crystal microbalance (QCM) into the lower reactor electrode. A general theory of the operation of a QCM can be obtained from the Maxtek manual or the general literature and will not be discussed here. The presence of the QCM apparatus within the plasma chamber allows real time acquisition of the rate of plasma polymer deposition within the reactor. With the system calibrated for a

particular monomer such as acetaldehyde, real time measurement of the plasma polymer thickness over time yields the rate of deposition.

One of the challenges of plasma polymerization is controlling both the outflow (from the vacuum pump/trap system) and the inflow of a reactive monomer. This system was used to study the deposition rate of acetaldehyde plasma polymers directly on the QCM crystal over a region of flow rates and RF power input settings. The reactor configuration was first calibrated for flow rate by allowing the system to reach an equilibrium monomer pressure (EMP), isolating the reactor from the pump and cold trap, and measuring the pressure rise of the system. Plotting the pressure vs. time yields a curve with an excellent linear fit as shown in Figure 1. The slope of the curve is used as the flow rate at the EMP, which is converted to flow at STP using equation 1. The flow rate at STP is then plotted vs EMP with an excellent fit to an equation with the form

$$F = a(EMP)^b \qquad \text{(Equation 2)}$$

as suggested by Yasuda,[7] where ***a*** and ***b*** are empirical factors. This data is shown for acetaldehyde in Figure 2. It should be noted that once the system is calibrated in this manner, if no changes in the configuration of the plasma system are made, the flow rate at STP can be calculated directly from the EMP and Equation 2.

The rate of plasma polymer deposition is obtained by initiating a plasma in the system at a given EMP and RF power settings and measuring the rate of deposition with the QCM. The stable linear portion of the deposition rate curve between 5 and 20 seconds were used, and the data were fit to a linear equation. Typical correlations using this method were between 0.92 and 0.99. Poorer correlations were obtained for the higher deposition rates due to the stepwise incremental signal of the QCM apparatus, giving rise to greater scatter in these curves. Plasma polymer deposition was performed over a number of RF power settings for a given EMP giving rise to a matrix containing EMP and RF power as the dependent variables and plasma polymer thickness as the independent variable. RF power settings between 5 and 80 W were used, with the limiting factor being the appearance of a bright spot in the reactor at an excessive RF power for a given monomer flow rate (where assumptions about the equilibrium deposition rate within the glow discharge area would clearly not apply).

Once a bright spot occurred for a given EMP, higher RF power settings were not used for that particular EMP since the plasma conditions were considered to be inhomogeneous.

The deposition rates obtained were then plotted vs the specific composite parameter of RF power/Flow rate (W/F). This is a contraction of the Yasuda parameter W/FM, where the molecular weight is included. Since only one monomer was studied in this system, the denominator is a constant and was therefore ignored. Plotted in this manner, the deposition rates formed a family of curves for each value of EMP vs. RF power employed, each of which could be empirically fit to an equation of the form

$$k = A\ln\left(\frac{W}{F}\right) + b \qquad \text{(Equation 3)}$$

with correlation coefficients between 0.977 and 0.990, as shown in Figure 3. Thus for a given EMP, a general equation for the prediction of the rate of deposition was obtained.

Discussion

The orderly nature and continuous transition from a nearly vertical slope for the curve with an EMP of 0.450, to the nearly flat curve for the EMP of 0.104 in Figure 3 implies that a more general equation may be found for the rate of deposition for a given EMP in the form of

$$k_i = A_i\ln\left(\frac{W}{F}\right) + b_i \qquad \text{(Equation 4)}$$

where A_i and b_i are terms corresponding to the i^{th} EMP value. Empirically, plotting the experimental A_i and b_i terms from the line fits in Figure 3 vs EMP yields two linear equations for the A_i and b_i values over the experimental range studied, as shown in Figure 4. Significant scatter in the data occurs with the points from the EMP of 0.450, which is a poorer logarithmic function fit as observed by the correlation coefficient.

The predicted values of deposition rate can be verified with data points from Figure 3. Using the parameters for the linear fit shown in Figure 4 to predict A_i and b_i for a given EMP, the calculated deposition rate agrees to approximately ten percent of

the measured deposition rate. Thus it appears that, although the terms for Equation 4 are derived empirically and are convolutions of the EMP through the flow rate as shown in Equation 2, this appears to be a reasonable method of obtaining an estimate of the rate of deposition of acetaldehyde for our system within the monomer flow rate and RF input power space explored.

It is also apparent from these results that, in the immediate case for acetaldehyde, there does not appear to be a clear demarcation between the monomer limited and power limited regions of plasma deposition rate as suggested by Yasuda[8]. Rather a smooth transition from the monomer limited region to the power limited region occurs. We somewhat expected to observe a clearer demarcation between these two regions, and would expect the change from a monomer limited to power limited region would occur at the same location on the W/F ordinate in Figure 3 for each family of curves, which does not appear to be the case. Additionally, there clearly is not a unique space of deposition rate vs. W/F for the single monomer examined here. Rather, the observed deposition rate is strongly dependent upon the flow rate of the monomer as expected, with each flow rate yielding a unique curve on the W/F axis.

It can be argued that the method of experimentation employed here using very low glow discharge equilibration times may indicate that the system is not steady state over the duration of the plasma polymerization conditions. Yasuda and Wang describe their methodology of equilibrating the plasma system for 30 minutes prior to measuring their rate of plasma polymerization[9]. However, in our work, practical considerations dictate that plasma polymer surface modifications be conducted for very short time periods, typically between 5 and 60 seconds. Thus the experimental considerations in this study have attempted to duplicate realistic plasma polymerization conditions that would be used in a commercial process for very thin plasma polymers for surface functionalization.

Conclusions

Incorporation of a QCM microbalance into a plasma reactor allows the direct measurement of plasma polymer deposition rates. With this system we have investigated the deposition rate of acetaldehyde plasma polymers for a range of monomer flow rates and RF power input. The rapid generation of a large amount of

rate data in this system yields empirical equations describing acetaldehyde plasma polymer deposition rates using the psuedo composite parameter W/F.

Acknowledgement: This work was performed while with CSIRO Chemicals & Polymers in Melbourne, Australia. Many thanks to Prof. Hans Griesser (U. Adelaide) for the opportunity to work on this project.

Figure 1. Linear fits for $(dp/dt)_{V,T}$ for acetaldehyde plasma polymers for different equilibrium monomer pressures. Correlation coefficients for each curve are shown adjacent to the respective EMP value.

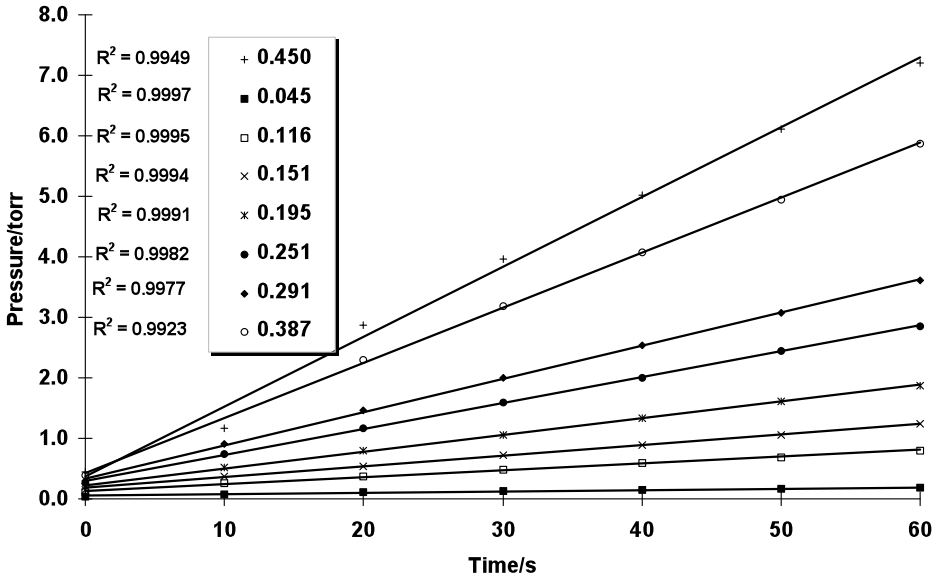

Figure 2. Flow rate at STP for acetaldehyde vs EMP. The exponentially fit equation to the data and correlation coefficient are also shown.

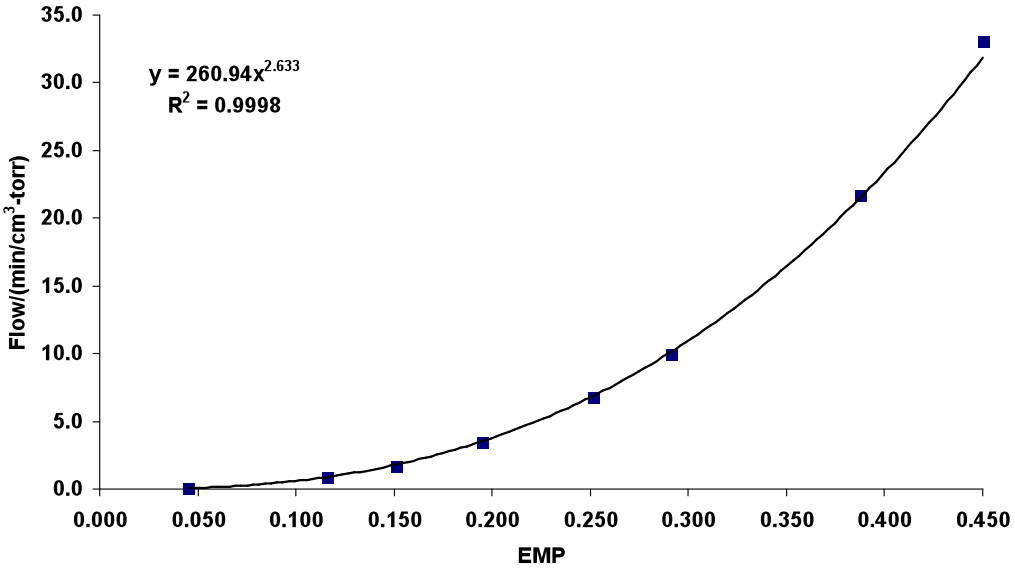

Figure 3. Deposition rates of acetaldehyde plasma polymers plotted vs. the psuedo composite parameter W/F for EMP values studied. Empirical equations of fit and correlation coefficients are also shown next to the respective curves.

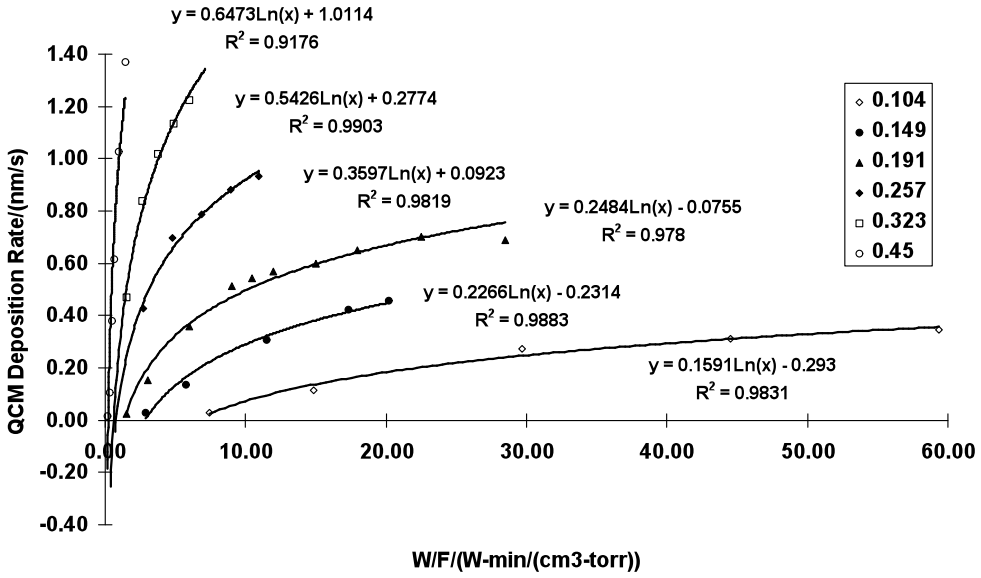

Figure 4. Linear fit of A_i and b_i terms from the equations shown in Figure 3 for the equations $Y = A_i*Ln(X) + b_i$.

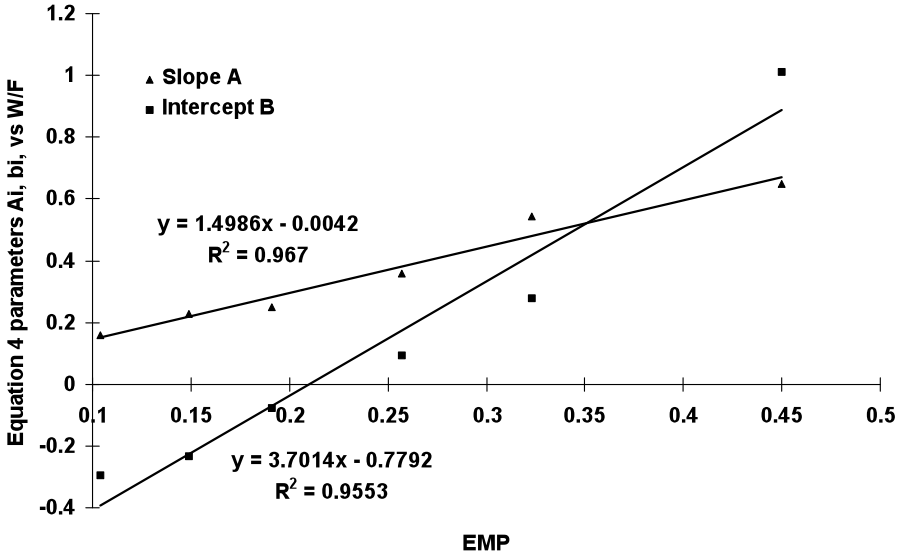

1 . Gerrit J. Beumer, Xiaoyi Gong, Liming Dai, Heather A.W. StJohn and Hans J. Griesser, Polymer Preprints 76, American Chemical Society Meeting.

2 . Borch, R.F., Bernstein, M.D., Durst, H.D., JACS, ***93(12)***, 2897-2904, (**1971)**.
3 . Evans, M.D.M., Xie, R.Z., Fabbri, M., Bojarski, B., Chaouk, H., Wilkie, J.S., McLean, K.M., Cheng, H.Y., Vannas, A., Sweeney, D.F., IOVS, 43(10), (**2002)**.

4 . T.R. Gengenbach, Z.R. Vasic, R.C. Chatelier and H.J. Griesser, *J. Polym. Sci.: Pt.A: Polym. Chem.*, ***32***, 1399 (**1994**).

5 . H.J. Griesser, *Vacuum*, ***39,*** 485 (**1989**).

6 . Yasuda, H., Plasma Polymerization, Academic Press, **1985**, Chapter 9, p. 278.

7 . Yasuda, Op. Cit., p. p.288.

8 . Yasuda, Op. Cit., Chapters 6, 8.

9 . Yasuda, H., Wang, C.R., J. Polym. Sci., Polym. Chem. Ed., ***23***, 87 (**1985**).